Automating 2D Suture Placement

Varun Kamat[1], Viraj Ramakrishnan[1], Yashish Mohnot[1], Harshika Jalan[1], Julia Isaac[1], Vincent Schorp[1,2]
Yahav Avigal[1], Aviv Adler[1], Danyal M Fer[3], Ken Goldberg[1]

2023 IEEE 19th International Conference on Automation Science and Engineering (CASE) | 979-8-3503-2069-5/23/$31.00 ©2023 IEEE | DOI: 10.1109/CASE56687.2023.10260435

***Abstract*— Suture placement is crucial for patient outcomes, and surgeons typically rely on rules of thumb and experience to choose needle entry and exit points for suture placement. In this paper we present SP2DEEF: Suture Planning 2D Equalizing Elliptical Forces, an algorithm that computes entry and exit points to optimize suture forces, improving wound closure and minimizing scarring. SP2DEEF takes as input the wound curve along with scaling information as input, and generates a full, optimized suture plan that can be fine-tuned by the surgeon. Experiments suggest that our suturing algorithm outperforms a naive baseline, and physical phantom experiments suggest that it performs comparably or superior to an expert surgeon.**

I. Introduction

Suturing is the process of sewing a wound or laceration closed to allow it to heal naturally. It is extremely common in surgery and trauma care and involves long sequences of precise, repetitive movements – something that is often burdensome to humans.

This work focuses on one aspect of automating suturing: the sub-task of *suture planning*, which is to find an appropriate sequence of needle insertion and extraction points. Having a high quality placement of suture is crucial for healing, as having sutures that are too close or tight may lead to ischemia (under-supply of oxygen to the tissue), while having sutures too far apart may lead to insufficient closing force on the wound to ensure the edges stay together [1]. Furthermore, sutures may exert shear forces along the wound, which cause more pronounced scarring and lead to cosmetically unappealing results [2] [3]. Thus, it is ideal to plan sutures by directly optimizing the forces they are expected to generate. Humans cannot directly estimate closure and shear forces as they suture, and typically rely on rules of thumb, intuition, and experience to guide suture placement.

This paper makes five contributions:

1) 1) A novel objective, optimizing Elliptical Force on the wound, based on an extension of the well-known "diamond force model" [4], [5] to nonlinear 2D wound shapes.
2) A novel formulation of planar, non-linear suture planning as a constrained optimization problem.
3) An analysis of the SP2DEEF algorithm's output on wounds of varying degrees and curvature.
4) Experiments comparing the suture placements from SP2DEEF to those chosen by a human surgeon.
5) An interactive interface that allows surgeons to upload an image, trace the wound curve, view proposed sutures and edit suture placement.

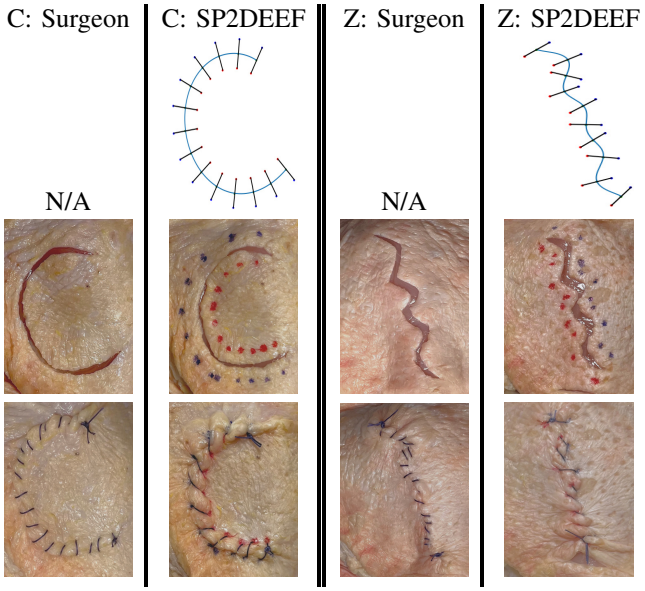

Fig. 1: Physical Experiments with chicken skin. Top row: SP2DEEF's outputted placements; Middle row: Surgeon's initial state and physical ink markings of SP2DEEF's placements; Bottom row: after suturing. Left half: C-shaped wound; Right half: Z-shaped wound. First and third columns: Surgeon's placement; second and fourth columns: SP2DEEF's placement. SP2DEEF's placements were evaluated as equal or better than the surgeon's placement by the surgeon.

II. Related Work

Automated and robot-assisted suturing has seen considerable study over the last decade, with particular focus on two sub-tasks: *2D suture planning*, which considers where to place sutures (the focus of this work), and *3D needle path planning*, which considers how to guide the needle to best accomplish a desired suture. Automating either of these sub-tasks can provide valuable assistance to a human surgeon, while having both may potentially lead to a fully automated suturing system.

A. Needle Path Planning

Much of the work on autonomous suturing focuses on needle path planning in the vertical plane (orthogonal to the wound line), as pushing a needle through deformable

The AUTOLAB at the University of California, Berkeley (automation.berkeley.edu)
[1] AUTOLAB at University of California, Berkeley
[2] Autonomous Systems Lab, ETH Zurich
[3] MD, Department of Surgery, University of California San Francisco East Bay

tissue represents a major challenge for sensing and control. In general, needle path planning focuses on a single suture at a time.

Nageotte et al. [6] proposed a kinematic analysis and geometric modeling of the problem of the stitching task in laparoscopic surgery. The work particularly uncovers the degree of uncertainty which the surgeon has with regard to where the tip of the needle is; that is, the exit point may not be exactly where desired.

Schulman et al. [7] applied the *transfer trajectory algorithm* to take trajectories from human demonstrations and adapt them to new environment geometry for suture needle path planning. Another approach developed by Sen et al. [8], was one of sequential convex optimization. As with the other papers, the optimization was over the execution of a single suture. Their approach considers multiple sutures, but the suture locations are chosen by linear interpolation of the start and end points, and each suture is treated independently thereafter. This method does not capture the constraints that the curvature of a wound might place on suture placement. Later, Shademan et al. [9] studied suturing on intestinal tissue. Various constraints for good suturing are discussed in this work: for instance, that sutures should be perpendicular to the wound, and the gaps between the sutures must be small enough to avoid leakage, but not too small as to prevent bloodflow. However, they are primarily used as assumptions that hold for a set of planned sutures that have been decided beforehand.

Other papers consider additional aspects of needle path planning: for example, Pedram et al. [10] presented an algorithm that takes in the desired suture entry and exit points on a wound as input and computes the needle shape, diameter and path so that the execution of the suture satisfies recommended suturing guidelines. These guidelines included: a minimization of tissue trauma, orthogonal sutures, positioning the needle to allow for successful grasps, suture symmetry and being able to enter and exit at the points defined by the surgeon. The optimization weights were selected based on the recommendation of surgeons and fine-tuned during simulations. Jackson et al. [11] proposed a Kalman filter to model the internal deformation force generated by a needle as it is driven through tissue. Similarly, Pedram et al. [12] described a needle stitch path planning algorithm which deals with optimal motion of the needle inside the tissue, with the goal of entering the tissue perpendicularly; reaching specific suture depth; and minimizing tissue trauma.

B. The Suture Planning Problem

There is prior work in planning the location of suture entry and exit points in the horizontal plane, for specific wounds, and in certain controlled settings. In particular, robotic minimally-invasive surgery (RMIS) must conform to the robot's kinematic constraints and the potentially very tight space in which the operation takes place.

Saeidi et al. [13] describe a planning algorithm for autonomous suturing using a segmented point cloud and demonstrated its application with the Smart Tissue Autonomous Robot (STAR) system. However, their technique assumed a straight-line wound (as can be expected in surgery, where the wound is the result of a surgical incision). Similarly, Thananjeyan et al. [14] studied suture planning for a circular wound. The primary constraints in both works were limitations to the robot's movement ability, either from kinematics or from a sharply bounded workspace, with the objective being to ensure evenly-spaced sutures with the gaps between them being as close as possible to an ideal distance.

However, when dealing with more complex wound shapes, sutures may interact with each other in more complex ways, and thus planning and evaluating an effective set of sutures may require a more detailed model of how the sutures hold the wound together.

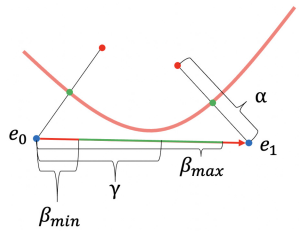

Fig. 2: Wound centerline shown in red, with two entry points (red) and two exit points (blue). Consider the distance between extraction points e_0, e_1. If the distance is between β_{min} and β_{max}, i.e. the green zone, it meets the constraints. Hence e_0 and e_1 violate constraints.

III. Problem Statement

Given an image with points along the wound selected by the surgeon, the suture planning problem consists of choosing the number and placement of sutures to best close the wound. We denote the number of sutures as n, and, for most of what follows, we treat it as fixed and consider the optimization problem which represents the task of finding the best placement of n sutures; we discuss how n is selected in Section IV-B. The parameters of this problem come in two types: the first type denote physical constraints or objectives. For example, the minimum allowable distance between any two skin puncture points or the ideal distance between the insertion and extraction points of a single suture (which we refer to as the *suture width*, α) We represent such constraints with Greek letters. The second kind of parameter are scalar weights which set the relative importance of different components of the objective function, and are represented by $c^\star$ where the superscript $\star$ denotes the corresponding component.

Let α be the *suture widths*, that is, the distance between the insertion and extraction points of a single suture. These two points are placed at equal distance apart from the wound such that their midpoint lies on the wound curve. Additionally, no two insertion and/or extraction points should be closer than a certain minimum distance, denoted $\beta_{\min}$, and no two consecutive insertion and/or extraction points should be further than a certain maximum distance, denoted $\beta_{\max}$. We also define the *suture distance* which is the straight line distance between the midpoints of two stitches. Guidance

for surgeons suggests that an ideal suturing distance is 5mm [15]. Let γ be this target distance between sutures, and let ℓ be the length of the wound.

Let L^d be the Mean Squared Error (MSE) defined as average difference between computed suture distance and the target suture distance γ. Let $L^{\text{var\_center}}$ be the variance of computed suture distances. Let $L^{\text{var\_ins\_ext}}$ be the variance of the distances between consecutive suture insertion and extraction points. In this term, we sum up the variance of the distance between insertion points and the variance of the distance between exraction points. Let L^f be the MSE between the closure force at each point along the wound curve and an ideal value. Similarly, Let L^{shr} be the MSE between the shear force at each point of the wound and an ideal value. Note that these target values are defined directly from the surgeon's input to the system.

Assume the suture planning is constrained to a given suture width α. Further assume that sutures are constrained to be orthogonal to the wound curve; therefore it is sufficient to specify the number n of sutures and at which points $0 \leq s_1 \leq \cdots \leq s_n \leq t_{\max}$ along the wound they are placed, to describe a complete suture plan of needle insertion and extraction points. Here, s_i serve as our decision variables (the center of suture i being $w(s_i)$). Additional we impose hard constraints that concern minimum and maximum distances allowed between consecutive insertion and extraction points. We denote these as constraints $A^{\min}, A^{\max}$. Finally, we enforce that sutures should not 'cross.' That is, if we draw a line from corresponding insertion point to extraction point for each suture, it should be the case that none of these lines are crossing. This constraint is denoted as A^c.

Each of the optimization terms $L^{\cdot}$ is weighted with a factor $c^{\cdot}$. The objective is then to find the sequence of s_i for all $i \in \{1, ..., n\}$ satisfying:

$$\begin{aligned} \min \quad & c^d L^d + \\ & c^{\text{var\_center}} L^{\text{var\_center}} + \\ & c^{\text{var\_ins\_ext}} L^{\text{var\_ins\_ext}} + \\ & c^f L^f + c^{\text{shr}} L^{\text{shr}} \qquad (1) \\ \text{s.t.} \quad & \\ & A^{\min}, A^{\max}, A^c \\ & 0 \leq s_1 \leq \cdots \leq s_n \leq t_{\max} \end{aligned}$$

Note that the number of sutures n is fixed in this problem; to minimize the loss over all possible suture plans, the problem needs to be solved with various different values of n, which we choose heuristically; see Section IV-B for details.

The objective function consists of three geometric cost terms (L^d, $L^{\text{var\_center}}$ and $L^{\text{var\_ins\_ext}}$) and two force model-based cost terms, both measuring the mean squared error. Its solution represents a sequence of suture midpoints which should be close to evenly spaced while also explicitly ensuring good closure forces over the wound. We will set the weights to emphasize L^f (closure forces), with the other components there to provide numerical stability and refinement.

See sections IV-C, IV-D and IV-E for a complete mathematical description of the objective function and constraints.

IV. Methodology

The SP2DEEF algorithm is divided into three distinct phases:

A. *Input*, in which the system queries the surgeon for points along the wound curve, desired suture width, and scaling information;

B. *Optimization with elliptical force model*, in which the system plans a set of sutures to minimize an objective function under constraints, utilizing an explicit model to estimate forces applied by the sutures to the wound;

C. *Adjustment*, in which the surgeon can optionally adjust the suture plan computed by the system.

A. Input

The interface first collects surgeon input, via a clicking interface, as depicted in Fig. 6. The surgeon selects two points on the image and inputs the measured distance between those points as well as the desired suture width.

The program scales the image based on the calibration points provided. The surgeon then clicks a sequence of points on the image tracing the shape of the wound. We then use the scipy interpolation function `scipy.interpolate.splprep` to generate a smooth B-spline that approximates a curve that goes through all points specified. We then generate an initial placement of sutures to 'warm start' the optimization. To that end, the algorithm computes the initial number of sutures by dividing the length of the wound curve by the ideal suture distance γ. It then places the corresponding number of equally spaced suture midpoints along the wound curve. The insertion and extraction points are determined by the perpendicularity constraint between the sutures and the curve as well as by the surgeon-specified suture width.

B. Optimization

SP2DEEF solves the placement of sutures on a wound as a constrained optimization problem. In order for the healing process to occur, the two sides of the wound must be brought together. Ideally, we would use a detailed model to predict skin deformation after suture placement. However, the mechanical behavior of skin is complex and influenced by the location on the body of the wound and the patient's height, weight, and age, amongst other factors, [1] making full modeling impractical. Instead of this, surgeons usually employ heuristics to plan where to place sutures. These heuristics state that sutures should be orthogonal to the wound, or that they should be spaced evenly and as close as possible to some ideal distance apart. However, relying exclusively on such rules can lead to solutions which leave parts of the wound insufficiently closed, because of insufficient closure force from sutures in the region. Thus, it is desirable to combine surgical heuristics with a model of the forces imparted by the sutures to ensure that the entire wound is held sufficiently closed by the sutures. This 'hybrid' optimization problem

leverages surgeons' experience while also ensuring that each point along the wound receives acceptable closure forces.

We assume that the wound lies on a 2D plane and place the sutures using only a 2D image of the wound as seen by an overhead camera; we assume that the wound has been positioned and rotated to minimize the distortion incurred by perspective effects. The wound is thus represented by a parametric spline computed by interpolating over points clicked by the surgeon on the image, which we denote as a function $w(t) = (x(t), y(t))$ where $w : [0, t_{\max}] \to \mathbb{R}^2$.

Since this optimization problem is in general nonconvex, we solve it with the SLSQP algorithm [16], which performs constrained optimization using linear approximation.

To find the best number n of sutures, we execute a bi-linear search from an initial naive estimation $\hat{n}$, as for a typical wound there is only a small range of 'reasonable' values of n. We use $\hat{n} = \lfloor \ell/\gamma \rfloor$, as this is the number of sutures resulting from naively spacing the sutures at distance γ along the length-ℓ wound, and is therefore likely to be close to the best number of sutures. We estimate ℓ via linear approximation and compute $\hat{n}$; then we solve the optimization problem (1) for all integers n such that $0.5 * \hat{n} \leq n \leq 1.4 * \hat{n}$ and return the suture plan with the lowest loss.

For evaluating the hyperparameter settings we use the same loss as our training loss.

C. Suture regularity constraints and objectives

The suture width α is given by the surgeon in the input phase of the process and the number of sutures n is selected by the algorithm. The other parameters $\beta_{\min}, \beta_{\max}, \gamma$, are assumed to be constant. For our experiments, we set these values based on consulting an expert in the field of surgery[1] These parameters are depicted in Fig. 2. We also include several key conditions for suture placement:

(i) All sutures should cross the wound at their midpoint and be orthogonal to the wound at that point.
(ii) Sutures should have width (distance between insertion and extraction points) of α.

The hyperparameters $\alpha, \beta_{\min}, \beta_{\max}, \gamma, \varepsilon$ are set via... Since in general these conditions cannot be perfectly satisfied, some conditions are hard-coded as constraints and others are encoded via penalty terms in the objective function. Conditions (i) (orthogonality of sutures to the wound) and (ii) (suture width) mean that if the suture crosses the wound at some $w(s)$, the insertion and extraction points are uniquely determined (up to swapping); therefore, as discussed above, our decision variables are the points $0 \leq s_1 \leq \cdots \leq s_n \leq t_{\max}$ along the wound at which we want the sutures to cross, with suture i crossing at $w(s_i)$. Since the wound w is represented as a B-spline, it has a well-defined derivative $w'(t) = (x'(t), y'(t))$ at each t. Then, interpreting $w(t), w'(t)$ as vectors in $\mathbb{R}^2$, the insertion and extraction points are

$$a^0(s_i), a^1(s_i) = w(s_i) \pm \frac{\alpha}{2} \begin{bmatrix} 0 & -1 \\ 1 & 0 \end{bmatrix} \frac{w'(s_i)}{\|w'(s_i)\|} \tag{2}$$

[1]we consulted our co-author Danyal Fer, MD, Department of Surgery, University of California San Francisco East Bay.

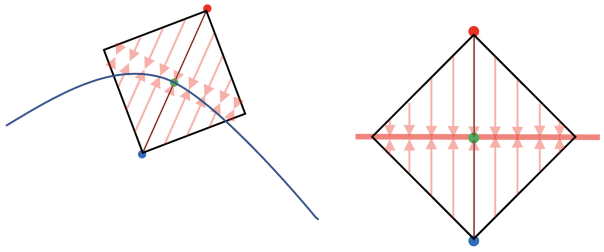

Fig. 3: **Diamond Force Model.**. The diamond model does not generalize well to non-linear wounds. As shown to the left, the curve pulls away from the diamond line, and thus it is non-obvious how to calculate distances.

Here a^0 corresponds to the insertion point and a^1 corresponds to the extraction point and both are vectors in $\mathbb{R}^2$. The side that corresponds to insertion and the side which corresponds to extraction was chosen arbitrarily and can be swapped if desired.

Conditions (iii) and (iv) are coded as the constraints labeled A^{crs} and $A^{\min}, A^{\max}$ respectively. A^{crs} states that for any $i \neq j$, the line segments $(a^0(s_i), a^1(s_i))$ and $(a^0(s_j), a^1(s_j))$ cannot cross; $A^{\min}$ states that no two different insertion and/or extraction points can be within $\beta_{\min}$ of each other; and $A^{\max}$ states that for any $i \in [0, n]$ and $z(\cdot) \in \{a^0(\cdot), a^1(\cdot), w(\cdot)\}$

$$\|z(s_{i+1}) - z(s_i)\| \leq \beta_{\max} \tag{3}$$

(no consecutive suture insertion points, extraction points, or midpoints can be more than $\beta_{\max}$ apart).

Condition (v) states that the distance between the sutures should be as close as possible to the ideal suture distance γ while condition (vi) ensures that the sum of variances of the insertion, center and extraction points is low. To measure how well a set of sutures satisfies conditions (v) and (vi), we use mean squared error and variance. To encode the constraint concerning the endpoints of the wound, we add 'phantom' sutures at $s_0 = 0$ and $s_{n+1} = t_{\max}$, giving:

$$L^{\text{idl}}(s_1, \ldots, s_n) = \sum_{z(\cdot)} \frac{1}{n+1} \sum_{i=0}^{n} (\|z(s_{i+1}) - z(s_i)\| - \gamma)^2 \tag{4}$$

$$L^{\text{var}}(s_1, \ldots, s_n) = \sum_{z(\cdot)} \text{Var}\left(\{\|z(s_{i+1}) - z(s_i)\|\}_{i=0}^{n}\right) \tag{5}$$

where $\sum_{z(\cdot)}$ indicates summing the function inside three times, with the points $z(s_i)$ being $a^0(s_i)$, $a^1(s_i)$ and $w(s_i)$, i.e. we take the average difference squared from ideal and the variance using the insertion points, the extraction points, and the midpoints and add them up. Conditions (i), (ii), (iii) and (iv) are treated as constraints while (v) and (vi) are encoded as penalty terms and in the objective function and optimized over.

D. Generalizing the Diamond Force Model

We supplement the suture regularity constraints and objectives with a model that aims to quickly estimate the forces applied by the sutures to the wound, inspired by the diamond force model [4], [5] on a linear wound, in which the force

imparted on the wound by a suture has a particular intensity at the crossing point and drops off linearly (to a minimum of 0) according to distance from the crossing point. An interesting feature of this model is that placing each suture at the point where the force from the previous suture drops to 0 yields a constant force across the wound. However, this model only considers linear wounds and does not generalize well when applied to curved wounds, as depicted in Fig. 3. We extend this to curved wounds by modifying it so that the forces imparted from an insertion or extraction point on the skin are parallel to the suture and decrease linearly (to a minimum of 0) based on an elliptical norm aligned with the suture. We choose an elliptical norm to represent the fact that the force of pushing on an elastic medium is transferred more strongly to points in line with the force than those to the side. We normalize the magnitude of the forces in our model by letting 1 unit of force be the ideal amount applied to close any given point on the wound, which is the amount applied by a suture to its midpoint. Since by symmetry the insertion and extraction points of a wound exert the same amount of force on the center, in opposite directions (since the suture center is the midpoint of the insertion and extraction points), this means that each insertion or extraction point exerts 0.5 units of force on its respective center. Thus, given a parameter $0 < \varepsilon \leq 1$ denoting the ratio of the shorter axis to the longer axis of the ellipse which defines the norm (to be discussed later), in our model the insertion point $a^0(s_i)$ has a suture-aligned distance from a point $z \in \mathbb{R}^2$ of

$$d^0(z,s_i) = \sqrt{d^0_{\parallel}(z,s_i)^2 + (d^0_{\perp}(z,s_i)/\varepsilon)^2} \tag{6}$$

where $d^0_{\parallel}(z,s_i)$ is the distance between $a^0(s_i)$ and z on the axis parallel to $a^1(s_i) - a^0(s_i)$ and $d^0_{\perp}(z,s_i)$ is the distance between $a^0(s_i)$ and z on the axis perpendicular to $a^1(s_i) - a^0(s_i)$; we define the distance $d^1(z,s_i)$ from the extraction point $a^1(s_i)$ analogously. Then, the force exerted on z from $a^0(s_i)$ is the vector

$$v^0(z,s_i) = \frac{1}{2} \frac{\max(\eta - d^0(z,s_i), 0)}{\eta - \alpha/2} \frac{a^1(s_i) - a^0(s_i)}{\alpha} \tag{7}$$

where $\eta = \sqrt{(\alpha/2)^2 + (\gamma/\varepsilon)^2}$. The force $v^1(z,s_i)$ imparted by an extraction point $a^1(s_i)$ on z is defined analogously. The suture force model is shown in Fig. 4. Note that the force vector is parallel to $a^1(s_i) - a^0(s_i)$ and (since $\alpha = \|a^1(s_i) - a^0(s_i)\|$ by definition) has the following properties: (a) $\|v^0(w(s_i), s_i)\| = 1/2$ for any i (insertion points, and by symmetry extraction points, exert a force of magnitude $1/2$ on the suture center); and (b) on a linear wound with sutures placed an ideal γ distance apart, each suture center lies on the boundary of the regions in which the previous and next suture exert forces of positive magnitude. We then set $\varepsilon = 0.77$ so that ideally-spaced sutures on a linear wound exert forces which are as constant as possible along the length of the wound. These properties extend the diamond force model to non-linear wounds.

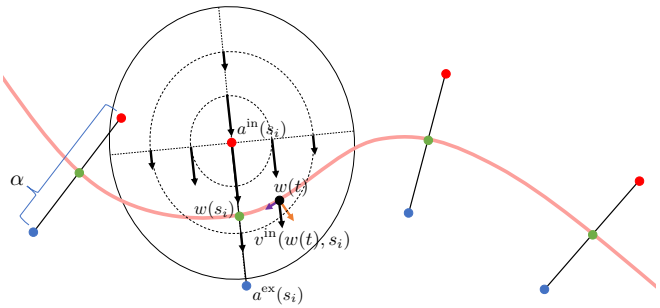

Fig. 4: **Elliptical Force Model.** Sutures (width α) with force model around insertion point $a^0(s_i)$ depicted as an ellipse showing the region of nonzero force imparted from $a^0(s_i)$, with forces decreasing linearly from the center, with isocontours of force being ellipses. Purple and orange arrows show shear and closure forces generated at the wound point $w(t)$ by $a^0(s_i)$.

E. Closure and shear force objectives

Given the model described in Section IV-D and Fig. 4 of how sutures exert force on skin, what does this imply about the quality of the sutures? While the insertion and extraction points are placed so that the suture (and thus the forces it exerts) are orthogonal to the wound at the crossing point, if the wound is not linear then at other points on the wound the exerted force may have both a *closure force* component orthogonal to the wound and a *shear force* component parallel to the wound. The total force exerted by insertion points (which push on one side of the wound) and the extraction points (which push on the other side of the wound) on $w(t)$, are denoted respectively as

$$F^0(t) = \sum_{i=1}^{n} v^0(w(t), s_i) \text{ and } F^1(t) = \sum_{i=1}^{n} v^1(w(t), s_i) \tag{8}$$

The total closure force at point $w(t)$ on the wound is:

$$f^{\text{c}}(t) = (F^0(t) - F^1(t))^{\top} \frac{a^1(s_i) - a^0(s_i)}{\alpha} \tag{9}$$

(note the $1/\alpha$ term to normalize the suture width). This value is normalized so that the ideal value is 1 at every $w(t)$.

To get the total shear force at a given point t on the wound, we take the components of the forces parallel to the wound:

$$f^{\text{s}}(t) = (F^0(t) - F^1(t))^{\top} \begin{bmatrix} 0 & -1 \\ 1 & 0 \end{bmatrix} \frac{a^1(s_i) - a^0(s_i)}{\alpha} \tag{10}$$

Since shear forces do not hold the wound together but may cause misalignment, the 'ideal' magnitude of the shear force is 0 at every t.

F. Force closure objective

We take m points $w(t_1), \ldots, w(t_m)$ and use the model above to estimate the closure and shear forces at these points. The average closure force penalty is then

$$L_{\text{c}} = \frac{1}{m} \sum_{j=1}^{m} (1 - f^{\text{c}}(t_j))^2 \tag{11}$$

(penalizing deviation from the ideal value of 1) and the average shear force penalty is

$$L_{\text{s}} = \frac{1}{m} \sum_{j=1}^{m} f^{\text{s}}(t_j)^2 \tag{12}$$

(penalizing deviation from the ideal value of 0). As with the regularity objective function, these components of the objective function are given weights c_c and c_s, respectively.

G. Parameter settings

We take α (suture width) as input from the user while we chose the values of $\beta_{\min}$, $\beta_{\max}$ (min and max distances between sutures) and γ (ideal distance between sutures) by consulting an expert in the field of surgery.

We developed the constraints using surgical suturing guidelines, setting $\beta_{\min} = 2.5$mm between two sutures as consulted by an expert surgeon[2] and $\beta_{\max} = 10$mm between consecutive sutures so as to not leave parts of the wound unclosed.

H. Adjustment

Finally, we provide a GUI for the surgeon to interact with. They are presented with the suture points, superimposed over the wound. The surgeon is able to drag the points to the desired place.

V. Experiments

A. Synthetic Splines

Our loss function contains weights on all 5 loss terms, which we manually tuned to the values: $c^d = 1$; $c^{var_center} = 12$; $c^{var_insext} = 6$; $c^f = 15$; $c^s = 5$.

Baseline Algorithm: We evaluate a baseline algorithm, which evenly places sutures along the curve spaced at the ideal distance, on the splines. This can be implemented by starting at one end of the wound, travelling the ideal distance along the wound, placing sutures at increments of the ideal distance until the end of the wound.

We tested both SP2DEEF and the baseline on 5 splines generated manually. To evaluate the robustness of the algorithms we created simple splines and splines with a higher degree and curvature. The suture placement points generated by the algorithms are depicted in Fig. 5. Our results show that the suture placements generated by SP2DEEF are relatively consistent, robust and well spaced, especially for the simpler splines. SP2DEEF also deals well with sharp curves (depicted in Spine 3) as it places a higher number of sutures close to the point of curvature.

SP2DEEF tended to choose a different number of sutures, when compared with the baseline. An optimal placement over an optimal number of sutures results in a lower closure force, while other terms tend to remain the same: the closure force that each suture exerts on the wound decreases sharply as the curve turns away from being perpendicular to the wound. To maintain sufficient closure force, it is necessary to increase the number of sutures. The baseline algorithm was not able to provide consistent closure force, as it is able to vary neither the number of sutures nor the placement to account for curvature.

While it reported high closure force losses, the baseline did well according to the variance and ideal distance metric, since it was initialized to be evenly spaced. The variances for the baseline aren't always 0, because we used a greedy algorithm which approximately placed sutures evenly. Furthermore, the insert and extract points may have additional variance on curved segments of the wound even if the centers are approximately evenly spaced.

One major improvement SP2DEEF saw was that it always avoided sutures crossing over and heavily penalized cases in which the sutures were placed too close to each other, in contrast to the baseline algorithm, which did both of these.

Overall, SP2DEEF outperforms the baseline; we believe that closure force is the most important metric as the main purpose of sutures is to provide closure forces to close a wound. Our algorithm finds a placement almost as well spaced as the baseline, with similar shear forces, while making sure that all the normalized closure forces are very close to the ideal. Although it does not outperform the baseline in the variance (and the shear sometimes), it makes up for this by returning a placement that optimizes the closure force.

B. Physical Experiments on Chicken Skin

We tested SP2DEEF in a physical experiment using chicken (thigh) skin. To find the most realistic wounds possible, we had a surgeon cut two wounds into the tissue with a scalpel[2]. These two wounds, as can be seen in Fig. 1, were chosen by the surgeon for their relevance to clinical wounds seen in practice, as well as their difficulty. As a baseline, we had a surgeon suture the wound as they saw fit. We then fed an image of the wound without sutures into our pipeline, clicked points to trace the wound shape, and recorded the optimized placement of the sutures, the output of our optimizer. We manually marked this placement on the phantom with ink, and had the surgeon implement the autonomous placement by suturing on top of the ink markings with USP Size 2-0 thread and a suture needle type GS-22 as depicted in Fig. 1.

Our placement was able to achieve wound closure on the phantom: we consulted an expert surgeon[2] who evaluated the sutures as equal or better than a human surgeon. In the test case, having SP2DEEF's placement marked on the skin helped the surgeon place sutures with consistent spacing throughout the whole wound. In contrast, in the baseline case, with no visual guides, the Surgeon stitches developed uneven spacing between suture locations as the wound was deformed during the suturing process.

VI. Conclusion

A. Limitations

This work has the following limitations:

- The wound is represented as a spline, and therefore the representation cannot have sharp corners (or branches).
- No information about the wound depth or width is incorporated.
- SP2DEEF assumes a fixed suture width as opposed to being able to modify it for particular sutures. Some better solutions may therefore be missed, particularly when tight wound curves are involved.

[2]We consulted our co-author Danyal Fer, MD, Department of Surgery, University of California San Francisco East Bay.

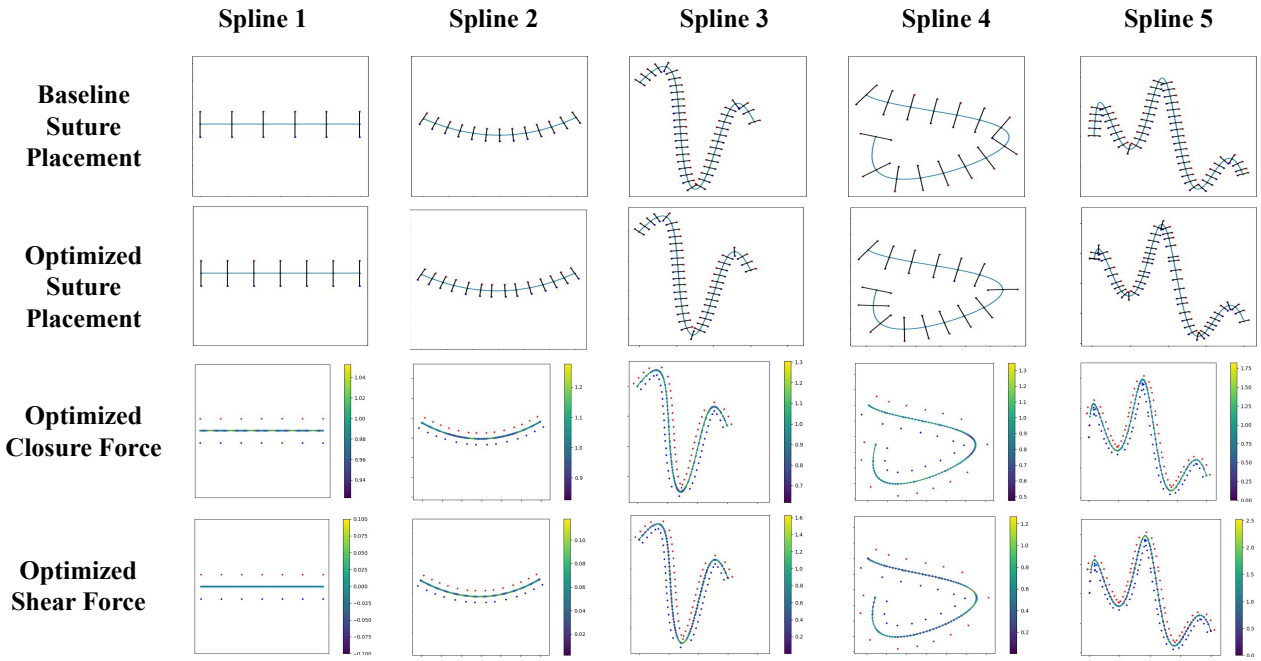

Fig. 5: Results analyzing the suture placements for 5 synthetic splines. Top two rows present the difference in the sutures placed using the baseline, as compared to the optimization algorithm. The bottom 2 rows present the shear forces and closure forces created by the optimization suture placement

TABLE I: Suture Placement Results

Loss Type	Algorithm	Spline 1	Spline 2	Spline 3	Spline 4	Spline 5
Variance - center points	Baseline	0.00	**0.02**	2.06	2.79	**0.77**
	Optimized Suture Placement	0.00	0.62	**1.51**	**1.24**	24.92
Variance - insertion / extraction points	Baseline	0.00	**0.05**	**28.12**	18.50	**47.66**
	Optimized Suture Placement	0.00	1.25	28.40	**13.65**	87.12
Ideal distance loss	Baseline	8.48	**5.34**	106.50	86.68	**185.58**
	Optimized Suture Placement	**4.50**	9.01	**64.88**	**25.95**	527.79
Closure Force loss	Baseline	3431.70	9410.64	9828.90	7776.41	8283.97
	Optimized Suture Placement	**0.61**	**5.68**	**0.01**	**0.00**	**9.54**
Shear Force loss	Baseline	0.00	54.86	**29.00**	104.66	**17.52**
	Optimized Suture Placement	0.00	**0.55**	39.13	**32.00**	113.43
Total loss (weighted)	Baseline	51483.98	141439.78	147878.44	117400.61	124827.93
	Optimized Suture Placement	**13.65**	**111.9**	**449.2**	**282.73**	**2059.8**
Number of Sutures	Baseline	6	13	40	15	51
	Optimized Suture Placement	7	14	39	15	53

- The explicit model of suture forces is only a rough approximation of how skin behaves under tension.
- No objective, external measure of suture placement quality was used to evaluate the algorithm.
- The sutures may be re-planned during the operation due to the wound changing shape when partially sutured.

B. *Future work*

Prior work on the suture planning problem focused primarily on achieving evenly placed sutures on known wound shapes under kinematic or workspace constraints. This suggests the possibility of combining such constraints with the wound-focused constraints and objective developed in this work, for instance by modifying the objective function to include a consistency measure and also account for the difficulty of executing the planned sutures.

REFERENCES

[1] D. L. Dunn, Ed., *Ethicon Wound Closure Manual*. Ethicon, Incorporated, 1994. [Online]. Available: https://books.google.com/books?id=BzG0PwAACAAJ

[2] D. Son and A. Harijan, "Overview of surgical scar prevention and management," pp. 751–757, 2014.

[3] N. Marsidi, S. A. Vermeulen, T. Horeman, and R. E. Genders, "Measuring forces in suture techniques for wound closure," *Journal of Surgical Research*, vol. 255, pp. 135–143, 2020. [Online]. Available: https://www.sciencedirect.com/science/article/pii/S0022480420303061

[4] J. G. Descoux, W. J. Temple, S. A. Huchcroft, C. B. Frank, and N. G. Shrive, "Linea alba closure: Determination of ideal distance between sutures," *Journal of Investigative Surgery*, vol. 6, no. 2, pp. 201–209, 1993, pMID: 8512892. [Online]. Available: https://doi.org/10.3109/08941939309141609

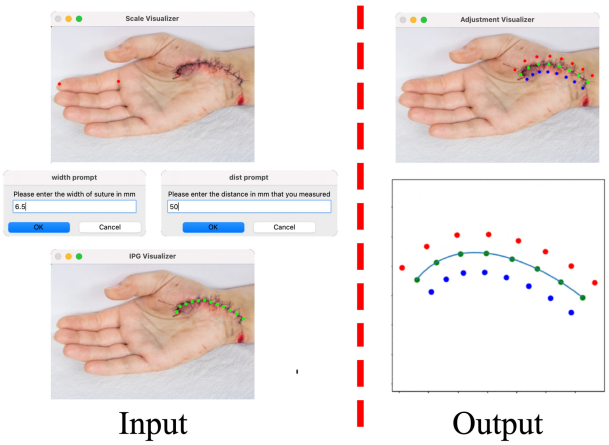

Fig. 6: **The full autonomous pipeline for optimizing surgical suture placement.**. Input: Surgeon selects two points on the image (finger length) and inputs the measured distance between those points as well as the desired suture width. The surgeon is further asked to click points along the wound. Output: The wound fitted as a Bézier curve (green) with the result of the suture optimization (red and blue points). The suture plan is overlaid on the original wound image.

[5] U. Devgan, "Basic principles of ophthalmic suturing," https://cataractcoach.com/2018/07/29/basic-principles-of-ophthalmic-suturing/, accessed: 2023-03-12.

[6] F. Nageotte, P. Zanne, C. Doignon, and M. de Mathelin, "Stitching planning in laparoscopic surgery: Towards robot-assisted suturing," *The International Journal of Robotics Research*, vol. 28, no. 10, pp. 1303–1321, 2009. [Online]. Available: https://doi.org/10.1177/0278364909101786

[7] J. Schulman, A. Gupta, S. Venkatesan, M. Tayson-Frederick, and P. Abbeel, "A case study of trajectory transfer through non-rigid registration for a simplified suturing scenario," *IEEE International Conference on Intelligent Robots and Systems*, pp. 4111–4117, 2013.

[8] S. Sen, A. Garg, D. V. Gealy, S. McKinley, Y. Jen, and K. Goldberg, "Automating multi-throw multilateral surgical suturing with a mechanical needle guide and sequential convex optimization," *Proceedings - IEEE International Conference on Robotics and Automation*, vol. 2016-June, pp. 4178–4185, 2016.

[9] A. Shademan, R. S. Decker, J. D. Opfermann, S. Leonard, A. Krieger, and P. C. W. Kim, "Supervised autonomous robotic soft tissue surgery," *Sci Transl Med*, vol. 8, no. 337, p. 337ra64, May 2016.

[10] S. A. Pedram, P. Ferguson, J. Ma, E. Dutson, and J. Rosen, "Autonomous suturing via surgical robot: An algorithm for optimal selection of needle diameter, shape, and path," *2017 IEEE International Conference on Robotics and Automation (ICRA)*, pp. 2391–2398, 2017.

[11] R. C. Jackson, V. Desai, J. P. Castillo, and M. C. Çavuşoğlu, "Needle-tissue interaction force state estimation for robotic surgical suturing," in *2016 IEEE/RSJ International Conference on Intelligent Robots and Systems (IROS)*. IEEE Press, 2016, p. 3659–3664. [Online]. Available: https://doi.org/10.1109/IROS.2016.7759539

[12] S. A. Pedram, C. Shin, P. W. Ferguson, J. Ma, E. P. Dutson, and J. Rosen, "Autonomous suturing framework and quantification using a cable-driven surgical robot," *IEEE Transactions on Robotics*, vol. 37, pp. 404–417, 4 2021.

[13] H. Saeidi, H. N. Le, J. D. Opfermann, S. Leonard, A. Kim, M. H. Hsieh, J. U. Kang, and A. Krieger, "Autonomous laparoscopic robotic suturing with a novel actuated suturing tool and 3d endoscope," *Proceedings - IEEE International Conference on Robotics and Automation*, vol. 2019-May, pp. 1541–1547, 2019.

[14] B. Thananjeyan, A. Tanwani, J. Ji, D. Fer, V. Patel, S. Krishnan, and K. Goldberg, "Optimizing robot-assisted surgery suture plans to avoid joint limits and singularities," *2019 International Symposium on Medical Robotics, ISMR 2019*, 2019.

[15] O. M. Education. (2016, Apr) Suturing techniques. [Online]. Available: https://oxfordmedicaleducation.com/clinical-skills/procedures/suturing-techniques/

[16] D. Kraft, "A software package for sequential quadratic programming," *Forschungsbericht- Deutsche Forschungs- und Versuchsanstalt fur Luft- und Raumfahrt*, 1988.